A&A 510, A94 (2010)
DOI: 10.1051/0004-6361/200912052

Astronomy & Astrophysics

Transit timing analysis of CoRoT-1b⋆ *(Research Note)*

Sz. Csizmadia[1], S. Renner[2,3], P. Barge[4], E. Agol[5], S. Aigrain[6], R. Alonso[4,7], J.-M. Almenara[8], A. S. Bonomo[4,9], P. Bordé[10], F. Bouchy[11], J. Cabrera[1,12], H. J. Deeg[8], R. De la Reza[13], M. Deleuil[4], R. Dvorak[14], A. Erikson[1], E. W. Guenther[8,15], M. Fridlund[16], P. Gondoin[11], T. Guillot[17], A. Hatzes[15], L. Jorda[4], H. Lammer[18], C. Lázaro[11,19], A. Léger[10], A. Llebaria[4], P. Magain[20], C. Moutou[4], M. Ollivier[10], M. Pätzold[21], D. Queloz[7], H. Rauer[1,22], D. Rouan[23], J. Schneider[12], G. Wuchterl[15], and D. Gandolfi[15]

[1] Institute of Planetary Research, DLR, Rutherfordstr. 2, 12489 Berlin, Germany
e-mail: szilard.csizmadia@dlr.de
[2] Institut de Mécanique Céleste et de Calcul de Éphémérides, UMR 8028 du CNRS, 77 avenue Denfert-Rochereau, 75014 Paris, France
[3] Laboratoire d'Astronomie de Lille, Université Lille 1, 1 impasse de l'observatoire, 59000 Lille, France
[4] Laboratoire d'Astrophysique de Marseille, UMR 6110, CNRS/Université de Provence, 38 rue F. Joliot-Curie, 13388 Marseille, France
[5] Department of Astronomy, University of Washington, Box 351580, Seattle, WA 98195, USA
[6] School of Physics, University of Exeter, Stocker Road, Exeter EX4 4QL, UK
[7] Observatoire de Genève, Université de Genève, 51 chemin des Maillettes, 1290 Sauverny, Switzerland
[8] Instituto de Astrofísica de Canarias, 38205 La Laguna, Tenerife, Spain
[9] INAF – Osservatorio Astrofisico di Catania, via S. Sofia 78, 95123 Catania, Italy
[10] Institut d'Astrophysique Spatiale, Université Paris XI, 91405 Orsay, France
[11] Institut d'Astrophysique de Paris, Université Pierre & Marie Curie, 98bis Bd Arago, 75014 Paris, France
[12] LUTH, Observatoire de Paris, CNRS, Université Paris Diderot, 5 place Jules Janssen, 92190 Meudon, France
[13] Observatório Nacional, Rio de Janeiro, RJ, Brazil
[14] University of Vienna, Institute of Astronomy, Türkenschanzstr. 17, 1180 Vienna, Austria
[15] Thüringer Landessternwarte, Sternwarte 5, Tautenburg 5, 07778 Tautenburg, Germany
[16] Research and Scientific Support Department, ESTEC/ESA, PO Box 299, 2200 AG Noordwijk, The Netherlands
[17] Observatoire de la Côte d'Azur, Laboratoire Cassiopée, BP 4229, 06304 Nice Cedex 4, France
[18] Space Research Institute, Austrian Academy of Science, Schmiedlstr. 6, 8042 Graz, Austria
[19] Departamento de Astrofísica, Universidad de La Laguna, 38205 La Laguna, Tenerife, Spain
[20] University of Liège, Allée du 6 août 17, Sart Tilman, Liège 1, Belgium
[21] Rheinisches Institut für Umweltforschung an der Universität zu Köln, Aachener Strasse 209, 50931 Köln, Germany
[22] Center for Astronomy and Astrophysics, TU Berlin, Hardenbergstr. 36, 10623 Berlin, Germany
[23] LESIA, UMR 8109 CNRS, Observatoire de Paris, UVSQ, Université Paris-Diderot, 5 place J. Janssen, 92195 Meudon, France

Received 12 March 2009 / Accepted 26 October 2009

ABSTRACT

Context. CoRoT, the pioneer space-based transit search, steadily provides thousands of high-precision light curves with continuous time sampling over periods of up to 5 months. The transits of a planet perturbed by an additional object are not strictly periodic. By studying the transit timing variations (TTVs), additional objects can be detected in the system.
Aims. A transit timing analysis of CoRoT-1b is carried out to constrain the existence of additional planets in the system.
Methods. We used data obtained by an improved version of the CoRoT data pipeline (version 2.0). Individual transits were fitted to determine the mid-transit times, and we analyzed the derived O–C diagram. *N*-body integrations were used to place limits on secondary planets.
Results. No periodic timing variations with a period shorter than the observational window (55 days) are found. The presence of an Earth-mass Trojan is not likely. A planet of mass greater than ∼1 Earth mass can be ruled out by the present data if the object is in a 2:1 (exterior) mean motion resonance with CoRoT-1b. Considering initially circular orbits: (i) super-Earths (less than 10 Earth-masses) are excluded for periods less than about 3.5 days; (ii) Saturn-like planets can be ruled out for periods less than about 5 days; (iii) Jupiter-like planets should have a minimum orbital period of about 6.5 days.

Key words. planetary systems – techniques: photometric – methods: numerical – occultations

1. Introduction

As a consequence of the gravitational perturbations, the mid-times of consecutive transits deviate from a linear ephemeris in a transiting exoplanet system (transit timing variation, hereafter

⋆ Based on observations obtained with CoRoT, a space project operated by the French Space Agency, CNES, with participation of the Science Programs of ESA, ESTEC/RSSD, Austria, Belgium, Brazil, Germany, and Spain.

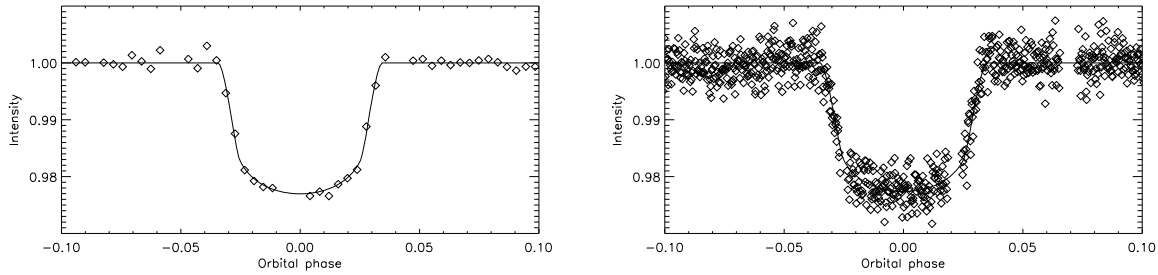

Fig. 1. *Top*: a typical transit observation of CoRoT-1b by CoRoT in the 512 s sampling rate mode. *Bottom*: a typical transit observation of CoRoT-1b by CoRoT in the 32 s sampling rate mode. Abcissa is phase, ordinate is normalized intensity. The solid lines show the fit.

TTV). Depending on the mass and the orbital configuration of the perturbing planet, this deviation can have amplitudes from a few seconds to days (e.g. Steffen 2006). Moreover, the duration, shape, and depth of the transits can also change. In extreme cases the transits can disappear and then reappear (Schneider 1994, 2004). Both the theoretical aspects and the observable effects have been studied in e.g. Miralda-Escudé (2002), Borkovits et al. (2003), Agol et al. (2005), Holman & Murray (2005), Ford & Holman (2007), Simon et al. (2007), Heyl & Gladman (2007), Nesvorný & Morbidelli (2008), Pál & Kocsis (2008) and Kipping (2009). Several transiting exoplanets were subject to this kind of analysis (Steffen & Agol 2005; Agol & Steffen 2007; Miller-Ricci et al. 2007; Alonso et al. 2009; Hrudková et al. 2008; Miller-Ricci et al. 2008a,b; Diaz et al. 2008; Coughlin et al. 2008; Rabus et al. 2009; Stringfellow et al. 2009).

In addition, stellar spots may affect the transit shape and, because of this, we have some difficulty in determining of the midtime of the transit. This effect may cause spurious periodic terms in the O–C diagram of exoplanets (Alonso et al. 2009; Pont et al. 2007).

Here we report the TTV analysis of CoRoT-1b based on data obtained by an improved version of the CoRoT data pipeline. In this system a low-density planet (mass: 1.03 $M_{\rm Jup}$, radius: 1.49 $R_{\rm Jup}$, average density: 0.38 g cm^{-3}, semi-major axis: 5.46 $R_\odot$, orbital period: 1.5089557 days) orbits a G2 main-sequence star (Barge et al. 2008). Thirty-six transits were observed by CoRoT, 20 of them in 512 s and 16 with the 32 s sampling rate mode. In total more than 68 000 data points were collected during 55 consecutive days (Barge et al. 2008). The operation of the satellite is described in detail in the pre-launch book, and the reader can find useful information about CoRoT in Baglin et al. (2007), Boisnard et al. (2006), and Auvergne et al. (2009).

2. Methods of mid-transit point determination: effect of the sampling rate on the precision

If one uses the CoRoT data for TTV analysis, the main limiting factor arises from the sampling rate. The typical length of the ingress/egress phase of a hot Jupiter is on the order of 10–20 min (in the particular case of CoRoT-1b, the ingress/egress time is 9.8 min) CoRoT targets are observed with 512 or 32 s sampling rates (the so-called undersampled/oversampled modes, see Fig. 1). Concerning a typical 3 h transit, one can easily conclude that a transit observation consists of only $(3 \times 3600\ {\rm s})/512\ {\rm s} \approx 21$ data points. In the oversampled mode we have typically over 300 data points per transit. The small number of data points in the undersampled mode may not be balanced by the very good photometric precision of CoRoT (which is about 0.1% for a 13 mag star in white light for a 512 s exposure, see Auvergne et al. 2009), therefore we chose to investigate this issue.

A second factor arises from the orbit of the satellite. The satellite periodically crosses the so-called South Atlantic Anomaly (SAA) region, which causes bad/uncertain data points and long data gaps (typically 10 min). This is significant only when the SAA-crossing occurs during the ingress or the egress phase. Therefore the following test was carried out. Using the exoplanet light curve model of Mandel & Agol (2002) and the parameters of the system (Barge et al. 2008), we simulated the light curve of CoRoT-1b. Then this curve was re-sampled to the same time-points as CoRoT observations. We added a Gaussian-like random noise to the points. The standard deviation of the noise term was chosen in such a way that we had the same signal-to-noise ratio as given in Barge et al. (2008) for the CoRoT-1 light curve. A constant orbital period was assumed.

Then we determined the mid-transit times in this simulated light curve, fitting each individual transit separately. Again, we use the Mandel & Agol (2002) model combined with the Amoeba algorithm (Press et al. 1992) to find the optimum fit. We assumed that the planet-to-stellar radius ratio and the limb-darkening coefficients are known, so they were fixed. The adjustable parameters are the mid-transit point, the inclination, and the $a/R_{\rm s}$ ratio (a: semi-major axis, $R_{\rm s}$: stellar radius).

On average, the fits of the individual transits yield only a difference of 9 s between the real and the determined midtransit points in the undersampled mode, when there are data points in the ingress/egress part of the light curve. When the ingress or egress part is missing in the undersampled mode, the errors can be as large as 20–60 s, depending on the distribution of points during the transit. If both the ingress and egress parts are missing, the errors are 60–120 s, sometimes even more.

These optimistic error bars should be increased due to at least two different effects. First, we do not know a priori the exact value of the orbital period which leads to small uncertainties in the calculation of the phase. We estimate that for CoRoT-1b this is negligible. Second, the stellar activity is not included. However, the detailed discussion of these two effects goes beyond the purpose of the present investigation.

Since we use a constant period and assume $e = 0$ during the simulation, we expect a linear O–C curve with some scatter. To better characterize this scatter we calculate the standard deviation of the sample. We find that the mean 1σ scatter of the resulting overall O–C diagram of this simulated light curve with a constant period is 22 s. But it is 27 s for the undersampled part and 16 s for the oversampled part.

3. TTV analysis of CoRoT-1b

We used the N2 level data points (Auvergne et al. 2009) processed by the 2.0 version of the pipeline (not yet realeased data

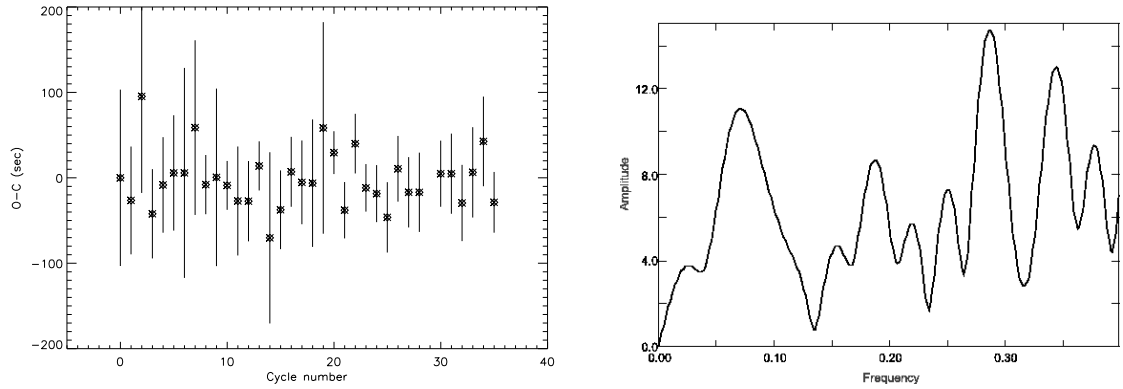

Fig. 2. *Top*: the O–C diagram of CoRoT-1b obtained by the light curve fit of the individual transits. *Bottom*: the power spectrum of the Fourier-transform of the O–C diagram. Frequency is in cycles/day and amplitude is in seconds.

Table 1. Mid-transit times (HJD) and errors (days) of CoRoT-1b.

HJD	Error (days)	HJD	Error (days)
2 454 138.32782	0.00039	2 454 165.48897	0.00028
2 454 139.83657	0.00024	2 454 166.99842	0.00047
2 454 141.34646	0.00043	2 454 168.50716	0.00019
2 454 142.85436	0.00020	2 454 170.01559	0.00025
2 454 144.36357	0.00021	2 454 171.52515	0.00026
2 454 145.87264	0.00025	2 454 173.03371	0.00021
2 454 147.38159	0.00047	2 454 174.54261	0.00025
2 454 148.89096	0.00039	2 454 176.05135	0.00031
2 454 150.39940	0.00013	2 454 177.56074	0.00029
2 454 151.90842	0.00039	2 454 179.06949	0.00031
2 454 153.41730	0.00010	2 454 180.57845	0.00035
2 454 154.92612	0.00024	2 454 183.59652	0.00029
2 454 156.43507	0.00018	2 454 185.10548	0.00035
2 454 157.94435	0.00011	2 454 186.61417	0.00034
2 454 159.45266	0.00038	2 454 188.12340	0.00040
2 454 160.96186	0.00017	2 454 189.63264	0.00040
2 454 162.47116	0.00015	2 454 191.14105	0.00027
2 454 163.98002	0.00018		

for the public). The resulting light curve was manually checked: a few data points were noted by the pipeline to be affected by cosmic ray events in spite of it having no problems – we restored these data points. In addition, several outliers were removed by hand. Then we performed a TTV analysis by fitting all transits using the method described in the previous section. Transit No. 30 is excluded from this investigation because it is strongly affected by noise. Table 1 gives the midtransit times and their errors.

The overall O–C diagram and its Fourier-transform are given in Fig. 2. This diagram is built using the observed light curve. It is prominent that after switching on the 32 s sampling rate mode (after the 20th transit), the 1σ scatter of the O–C diagram is reduced to only 18 s, compared to the 1σ scatter of the 25 s observed in the undersampled mode. The 1σ scatter of the whole O–C diagram is 22 s. All these scatter values are very close to the value we would expect in the case of a constant orbital period (see previous section).

No clear periodicity or trend can be identified in this diagram. We calculate the Fourier-spectrum of the O–C curve by the Period04 software (Lenz & Breger 2005) to search for any non-obvious periodicity. The power spectrum shows few peaks, but none of them is above the noise level. The highest peak has only $S/N \approx 2$, so it is not regarded as a real signal.

Table 2. Amplitudes and periods of O–C variations in CoRoT-1b system.

Mass of the perturbing object	Configuration	Amplitude in seconds	Period[1]
1 Earth mass	at L_4 point, 20° libration amplitude	60	~10
1 Earth mass	initially on circular orbit, 2:1 exterior mmr	100	~150
30 Earth mass	outer planet initially with $e = 0.05$ and $P = 2.277218632$ days	150	~15
30 Earth mass	outer planet initially with $e = 0.25$ and $P = 4.2679123$ days	150	~30

Notes. [(1)] In the units of consecutive transit numbers.

We conclude that there are not any periodic TTVs in CoRoT-1b with a period less than the observational window (55 days) and an amplitude larger than about 1 min (=3σ detection level). We also note that there is no significant change in the inclination and the $a/R_{\rm star}$ ratio during this interval. Bean (2009) presents results about the TTV analysis of CoRoT-1b based on the public data processed by an earlier version of the pipeline. His O–C diagram shows a larger 1σ-scatter (36 s compared to our 22 s).

4. Limits on secondary planets

4.1. Examples of simulated TTVs

We show in Table 2 which amplitudes and periods can typically be expected in the O–C diagram of the CoRoT-1b system based on some dynamical simulations. We include an Earth-mass planet at the L_4 Lagrangian point, an Earth in the 2:1 exterior mean motion resonance, a nearby Neptune-like planet, or an outer eccentric Neptune. The stellar mass, the mass of CoRoT-1b and its orbital elements are fixed to the values given in Barge et al. (2008). We use the Mercury software (Chambers 1999), with the Burlish-Stoer algorithm (accuracy parameter $\delta = 10^{-16}$). As one can see in Table 2, O–C variations on the order of 60–150 s might occur on a short time scale (typically 10–150 orbital cycles of the transiting planet).

Case 1: an Earth-mass Trojan planet librating with an amplitude of 20° around the L_4 Lagrangian point would have an amplitude of 60 s in the O–C diagram with a period of about 10 orbital cycles of the transiting planet (about 15 days, see Table 2). The

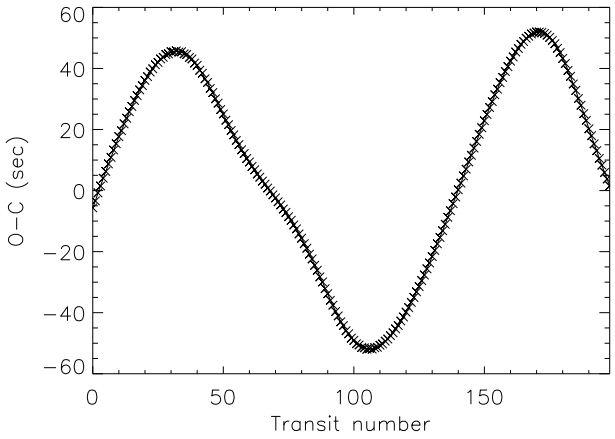

Fig. 3. The simulated O-C diagram of CoRoT-1b if the transiting planet is perturbed by an Earth-mass planet initially on a circular orbit in 2:1 mean motion resonance.

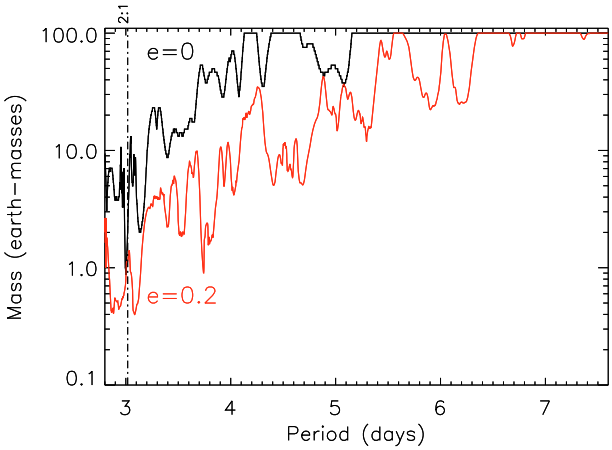

Fig. 4. Maximum allowed mass of a hypothetical perturbing object as a function of its orbital period for excentricities $e = 0$ and 0.2. The 2:1 mean motion resonance is indicated.

amplitude is close to our detection limit. There is a peak in the Fourier-spectrum of the O–C diagram at the corresponding frequency with an amplitude of about 11 s. However, the peak is not significant ($S/N = 1.3$ only). Therefore, an additional planet with similar parameters is not likely.

Case 2: an Earth-mass planet initially on a circular orbit and in 2:1 mean motion resonance with CoRoT-1b would have an amplitude of about 100 s in the O–C diagram with a period of about 150 transits (approximately 225 days, see Table 2 and Fig. 3). If the CoRoT observational window was around the maximum or the minimum of the O–C curve (see Fig. 3) then we would have no chance to discover this possible planet because the amplitude is on the order of the scatter. If the observational window matched the steepest part of the O–C diagram, we would observe a linear O–C curve that could be interpreted as a wrong period value. This gives a hint: if there are no observed period variations in a short observational window, this does not mean that we can give an upper limit for a hypothetical perturber object. It might be the case that we are on a linear part of the O–C curve. The observational window should be long enough to exclude similar cases.

Cases 3 and 4: simulations show that an outer 30 Earth-mass planet, close to CoRoT-1b ($P = 2.772118632$ days and $e = 0.05$) or eccentric ($P = 4.2679123$ days and $e = 0.25$), cause O–C variations of about 150 s, within approximately 15 and 30 orbital revolutions of the transiting planet, respectively (see Table 2). This is much greater than our detection limit, so outer planets in the CoRoT-1b system with similar orbital parameters can be excluded.

4.2. Detailed analysis

Using N-body integrations, we computed the maximum mass of a hypothetical perturbing planet, with given initial orbital periods and eccentricities, leading to TTVs compatible with the data. To calculate the transit times, we used a bracketing routine from Agol et al. (2005). The orbits of CoRoT-1b and an additional planet were computed over the timespan of the observations, using a Burlish-Stoer integrator with an accuracy parameter $\delta = 10^{-16}$. The equations of motion were integrated in a Cartesian reference frame centered on the barycenter of the system. The transit times are subtracted from the data to give the O–C residuals and χ^2.

The masses of the central star and CoRoT-1b are respectively fixed at 0.95 solar masses and 1.03 Jupiter masses (Barge et al. 2008). The orbit of CoRoT-1b is initially circular with an orbital period $P = 1.5089557$ d (Barge et al. 2008) and a true longitude $\theta = 0$ deg. With these parameters and without any perturbation due to an additional body, the first transit occurs at $T(HJD) = 2454138.327840$, and the residuals given by the numerical integration are at their minimum (i.e. the same as the ones from the best constant period fit, see Sect. 3) with the following values: zero mean, standard deviation $\sigma_{\rm min} = 21.62$ s, $\chi^2 = 24.55$.

The perturbing planet is assumed to be in the same plane as CoRoT-1b. For given initial orbital parameters, we increase the mass of the test planet, starting at 0.1 Earth masses, and calculate the standard deviation of the O–C residuals. We store the mass value for which this rms exceeds the observed scatter $\sigma_{\rm min}$. In this way we determine the maximum planet's mass allowed. The results are shown in Fig. 4 (respectively Fig. 5), which shows the maximum mass for a perturbing object as a function of its initial orbital period (resp. initial orbital period and eccentricity). In Fig. 4, the mass of the secondary planet has been varied between 0.1 and 100 Earth masses (100 values on a log scale), and its initial orbital period between 2.8 and 7.6 days (with a step of 0.0015 days). For any given orbital period, eccentricity, and mass value, the TTV-signal is computed over the range of possible initial true anomaly and longitude of pericenter values to minimize the resulting residuals. In Fig. 5, the perturbing planet is initially at its apocenter (fixed at 180 degrees from CoRoT-1b), and the following grid of parameters has been used: (i) masses between 0.1 and 100 Earth masses (100 values on a log scale); (ii) orbital periods between 2.8 and 7.6 days (with a step of 0.001333 days); (iii) eccentricities between 0 and 0.25 (100 values on a log scale).

From Fig. 4, Saturn-like planets can be ruled out for periods less than about 5 days if $e = 0$ (respectively 6 days if $e = 0.2$). As shown in the figures, perturbing planets with eccentric orbits obviously cause larger TTVs, hence have lower mass limits. Super-Earths are defined as planets with 1–10 Earth masses (Valencia et al. 2007). Depending on the initial eccentricity, such planets with orbital periods less than 3.4–4.1 days can be excluded. Planets with masses greater than 0.3–1.0 Earth masses can be ruled out by the data if they are in the 2:1 (exterior) mean motion resonance with CoRoT-1b. The data do not allow strongly constraining the mass of perturbing planets

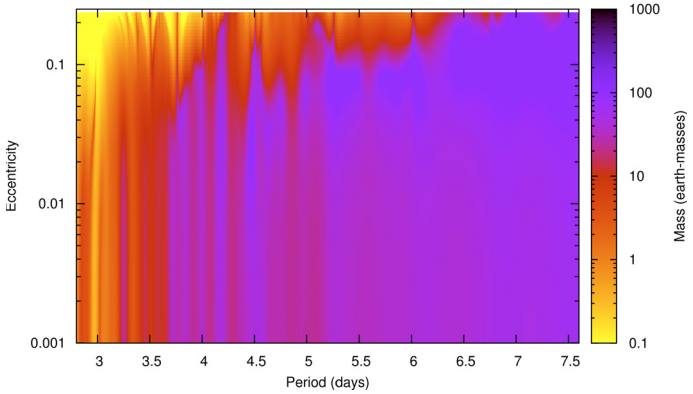

Fig. 5. Upper mass limits for a hypothetical second object in the CoRoT-1b system as a function of the perturber's orbital period and eccentricity.

near higher order resonances. Finally, we estimate the minimum orbital period for an outer Jupiter-mass planet. From Holman & Murray (2005),

$$M_{\rm perturber} = \frac{16\pi}{45} M_{\rm star} \frac{\Delta t_{\rm max}}{P_{\rm transiting}} \left(\frac{P_{\rm perturber}}{P_{\rm transiting}} \right)^2 (1 - e_{\rm perturber})^3. \quad (1)$$

When assuming a circular orbit and $\Delta t_{\rm max} = 3\sigma_{\rm min}$, this yields a minimum orbital period of 2.0 days. Otherwise, we would see its effect in the O–C diagram. This lower limit is in good agreement with the numerical simulations (see Figs. 4 and 5).

5. Summary

Our work shows that CoRoT allows study of the short time scale (30 days for the Short Run fields, 150 days for the Long Run fields) transit timing variations whose 1σ detection limit depends on the sampling rate, and it is 22 s for CoRoT-1b. The comparison of the O–C diagram of CoRoT-1b with numerical integrations leads to the following results: (i) an Earth-mass planet at the L_4 point is not likely. If existing, its detectability would be close to the 3σ detection limit, (ii) an outer Earth-mass planet in 2:1 resonance with CoRoT-1b can be rejected, given our data set. However, a longer observational window is required to fully assess the presence of such a planet, (iii) super-Earths are excluded for periods less than about 3.5 days, (iv) Saturn-like planets are ruled out for periods less than about 5 days.

Bean (2009) finds that there is no additional planet in the system with 4 Earth-mass or greater on an orbit with 2:1 mean motion resonance. Using an improved version of the CoRoT data pipeline, we confirm his result.

We also showed that TTV analyses of CoRoT data are promising for detecting additional objects in transiting systems observed by the satellite.

Acknowledgements. The team at IAC acknowledges support by grant ESP2007-65480-C02-02 of the Spanish Ministerio de Ciencia e Innovación. The German CoRoT Team (TLS and Univ. Cologne) acknowledges DLR grants 50OW0204, 50OW0603, and 50QP07011. E.A. thanks NSF for CAREER grant 0645416.

References

Agol, E., & Steffen, J. 2007, MNRAS, 374, 941
Agol, E., Steffen, J., Sari, R., & Clarkson, W. 2005, MNRAS, 359, 567
Alonso, R., Aigrain, S., Pont, F., T., et al. 2009, in Transiting Planets, Proc. IAU Symp., 253, 91
Auvergne, M., Bodin, P., Boisnard, L., et al. 2009, A&A, 506, 411
Baglin, A., Auvergne, M., Barge, P., et al. 2007, in American Institute of Physics Conference Series, 895, ed. C. Dumitrache, N. A. Popescu, M. D. Suran, & V. Mioc, 201
Barge, P., Baglin, A., Auvergne, M., et al. 2008, A&A, 482, 17
Bean, L. J. 2009, A&A, 506, 369
Boisnard, L., Baglin, A., Auvergne, M., Deleuil, M., & Catala, C. 2006, in ESA SP, 1306, 465
Borkovits, T., Érdi, B., Forgács-Dajka, E., & Kovács, T. 2003, A&A, 398, 1091
Chambers, J. E. 1999, MNRAS, 304, 793
Coughlin, J. L., Stringfellow, G. S., Becker, A. C., et al. 2008, ApJ, 689, 149
Díaz, R. E., Rojo, P., Melita, M., et al. 2008, ApJ, 682, 49
Ford, E. B., & Holman, M. J. 2007, ApJ, 664, 51
Heyl, J. S., & Gladman, B. J. 2007, MNRAS, 377, 1511
Holman, M. J., & Murray, N. W. 2005, Science, 307, 1288
Hrudková, M., Skillen, I., Benn, Ch., et al. 2008, in Transiting Planets, Proceedings of the International Astronomical Union, IAU Symp., 253, 446
Kipping, D. M. 2009, MNRAS, 392, 181
Lenz, P., & Breger, M. 2005, CoAst, 146, 53
Mandel, K., & Agol, E. 2002, ApJ, 580, 171
Miller-Ricci, E., Rowe, J. F., Sasselov, D., et al. 2007, ASPC, 366, 146
Miller-Ricci, E., Rowe, J. F., Sasselov, D., et al. 2008a, ApJ, 682, 586
Miller-Ricci, E., Rowe, J. F., Sasselov, D., et al. 2008b, ApJ, 682, 593
Miralda-Escudé, J. 2002, ApJ, 564, 1019
Nesvorný, D., & Morbidelli, A. 2008, ApJ, 688, 636
Pál, A., & Kocsis, B. 2008, MNRAS, 389, 191
Pont, F., Gilliland, R. L., Moutou, C., et al. 2007, A&A, 476, 1347
Press, W. H., Teukolsky, S. A., Vetterling, W. T., & Flannery, B. P. 1992, Numerical recipes (Cambridge University Press)
Rabus, M., Deeg, H. J., Alonso, R., Belmonte, J. A., & Almenara, J. M. 2009, A&A, 508, 1011
Schneider, J. 1994, P&SS, 42, 539
Schneider, J. 2004, ESASP, 538, 407
Simon, A., Szatmáry, K., & Szabó, Gy. M. 2007, A&A, 470, 727
Steffen, J. H. 2006, Ph.D. Thesis, University of Washington
Steffen, J. H., & Agol, E. 2005, MNRAS, 364, 96
Stringfellow, G. S., Coughlin, J. L., López-Morales, M., et al. 2009, in Cool Stars, Stellar Systems and the Sun, Proceedings of the 15th Cambridge Workshop on Cool Stars, Stellar Systems and the Sun, AIP Conf. Proc., 1094, 481
Valencia, D., Sasselov D. D., & O'Connell, R. J. 2007, ApJ, 656, 545